

# OPTIMISATION OF A SIFT DESCRIPTOR FOR FEATURE MATCHING

*Nicolas Hafner, Costanza Maria Improta, Zsombor Kalotay, Jan Leutwyler*

Department of Computer Science  
ETH Zürich  
Zürich, Switzerland

## ABSTRACT

The Scale Invariant Feature Transform is used to detect important regions in an image and allows tracking of such regions across transformed variants of the same image. We examine an existing implementation of the SIFT algorithm in C++ and compare it to our own in C. Our own implementation presents a cleaner interface, and manages to outperform the original C++ implementation in every substep of the algorithm. Using AVX2 vectorisation and other optimisation techniques we achieve speedups of up to 10x in select parts of the algorithm.

## 1. INTRODUCTION

### Motivation

The SIFT algorithm can be used for object recognition and object tracking, both important aspects of computer vision. The features it recognises in an image are robust against affine transformations, and even against variations in lighting. This is useful to recognise objects in video and track them as they move over time. Among other applications it can also be used for image stitching by aligning features with similar descriptors. Especially for the use in robotics and other real-time environments such as camera tracking, an efficient implementation of SIFT is important.

Optimisation of SIFT is non-trivial as it is a rather complicated algorithm to begin with. Many

of its steps also require a large amount of data access, sometimes over many different sets of data at once, complicating access locality.

In this work we first designed a reasonable architecture for SIFT that is amenable for future optimisations. We then wrote a straightforward implementation of SIFT in this architecture, including an automated test suite for verification and performance measurement. From there we performed both standard C optimisations as well as manual single-core vectorisation using AVX2, measuring and comparing along the way. In this paper we discuss and describe our methods and results.

### Related work

The original SIFT algorithm is outlined in a paper by Lowe [1][2].

Our implementation is based on the ezSIFT implementation by Wang [3] as well as the implementation in OpenCV[4]. Our own implementation is standalone like ezSIFT, but offers a pure C interface that can be used by any other project or language that supports the C calling convention. We also do not depend on any particular image format, but instead leave the loading of image data up to the user.

EzSIFT was chosen as a comparison point as it claims to be faster than the SIFT implementations of both OpenCV and VLfeat.

## 2. BACKGROUND

In this section we will outline the steps of the SIFT algorithm as detailed in the original paper[1], as well as our overall analysis of the algorithm in terms of asymptotic complexity and cost.

### The SIFT Algorithm

Our implementation of the SIFT algorithm is based on the work by Lowe [1], EZSift[3], and OpenCV[4]. The algorithm can be split into four stages.

The first stage is the *Scale-space Extrema Detection*. Here the scale space of an image is defined as a function  $L(x, y, \sigma)$ , that is produced from a convolution of a Gaussian kernel  $G(x, y, \sigma)$  with an input image  $I(x, y)$

$$L(x, y, \sigma) = G(x, y, \sigma) * I(x, y) \quad (1)$$

To efficiently detect extrema in scale space, a difference-of-gaussian pyramid is generated, where  $k$  represents a constant multiplicative factor

$$D(x, y, \sigma) = L(x, y, k\sigma) - L(x, y, \sigma) \quad (2)$$

To detect local minima and maxima in  $D(x, y, \sigma)$ , each pixel is compared to all 8 neighbours in the same scale, as well as to each 9 neighbours in the scale above and below of the pyramid.

The second stage is *Keypoint Localization*. In this stage a Taylor Expansion of the scale-space function  $D(x, y, \sigma)$  is used to determine the interpolated location and the scale of the extrema candidates. Also, final keypoints are selected based on measures of their stability. Hence, edge responses are eliminated to guarantee a high measure of stability.

The third stage is the *Orientation Assignment*. Here, one or more orientations are assigned to each keypoint location based on local image gradient directions. Pixel differences are used to calculate gradient magnitude  $m(x, y)$  and

orientation  $\Theta(x, y)$  from the Gaussian pyramid.

$$P(x, y) = L(x + 1, y, \sigma) - L(x - 1, y, \sigma) \quad (3)$$

$$Q(x, y) = L(x, y + 1, \sigma) - L(x, y - 1, \sigma) \quad (4)$$

$$m(x, y) = \sqrt{P(x, y)^2 + Q(x, y)^2} \quad (5)$$

$$\Theta(x, y) = \arctan \frac{Q(x, y)}{P(x, y)} \quad (6)$$

Then, an orientation histogram is formed from the gradient orientations of sample points within a region around the keypoint. This histogram has 36 bins covering the 360° range of orientations. Each sample added to the histogram is weighted by its gradient magnitude. Peaks correspond to dominant directions of local gradients.

The fourth and final stage is the *Extraction of the Keypoint Descriptor*. In the previous stages, an image location, a scale, and an orientation were assigned to each keypoint. As a last step, a highly distinctive descriptor for the local image region is computed. This descriptor is also as invariant as possible to remaining variations (e.g., illumination). This is achieved by taking a 16x16 pixel patch around a keypoint, subdividing this patch into 16 4x4 blocks, and, for each of these smaller blocks, creating an 8-bin orientation histogram. This histogram is used to form the keypoint descriptor.

### Cost Analysis

We analysed the algorithm precisely using a counting system. We separately considered floating point adds, muls, divs, and the amount of memory transferred. You can find the counts for a sample image tabulated in Table 1. Precise counts for all variants of our implementation and all image sizes are included in the source repository[5]. We make use of this counting scheme in order to automatically generate

the performance and roofline plots shown in [section 4](#). The counting facility is described in more detail in [section 3](#).

A precise asymptotic analysis of the algorithm is very involved, and can be found in a paper by Vinukonda [6].

### 3. OUR METHOD

With the background of the algorithm covered, we will now detail our implementation, which we call "ethSIFT" for short.

#### Testing and Measurement Framework

In order to verify the continued correctness of ethSIFT over the optimisation steps, and in order to conveniently measure the performance of the individual algorithm steps, we implemented a custom testing and measurement framework. In this framework, a new test can be defined using a special macro, `define_test`. The macros `with_measurement` and `with_repeating` allow convenient definition of regions that should be considered for measurement within the test, and finally the macro `fail` can be used to signal a test failure and give an appropriate description. An example test definition is shown in 1.

```
define_test(SampleTest, 1, {
    if(!prepare_things())
        fail("Test setup failed");
    with_repeating(compute_something());
})
```

Listing 1: A sample measurement test definition.

`with_repeating` automatically sets up a warmup loop followed by a loop of measurements of its body. Depending on the presence of the `USE_RDTSC` preprocessor flag, a measurement section will either measure the runtime using C++ `std::chrono`, or the cycle count using the `rdtsc` instruction. This allows us to measure both in separate runs with minimal noise, without

having to manually change or duplicate any of our code.

The tester framework automatically picks up any test definitions runs them in order of definition. For tests that incur measurement, the measurement values are automatically recorded, and the resulting median and median absolute deviation are output to CSV for plotting.

In order to capture accurate counts of flops and memory use, we also defined a custom set of macros that can be used to increase a relevant counter. We then manually invoke these macros throughout our code base whenever we explicitly perform a flop or access memory. These counters are only active when compiled with the `IS_COUNTING` flag, to avoid disturbing normal operations of the library. The counter values are output to a separate CSV file for processing in our plot system.

#### Overall Architecture

The overall architecture of ethSIFT was designed to allow allocations to be factored out of the primary loops as much as possible, and to allow the user more control over the individual steps where necessary. To this end, every step in the SIFT algorithm has a corresponding function in ethSIFT. To minimise heap access, all function arguments that are used as input are passed by value, including image structures. The return value of all ethSIFT functions is normalised to be a success value, though this is only really meaningful for functions that can fail.

We use a global initialisation function to precompute shared values such as the Gaussian kernels and temporary memory regions. We also provide an image pyramid allocation function that allows allocating all images of a pyramid in adjacent memory. This can be used to pre-allocate the pyramids and re-use them during multiple SIFT analysis runs. With pre-allocated pyramids, the SIFT algorithm does not require any further heap allocations during

Step	Adds	Mults	Divs	Bytes Transferred
Downscale	0	0	0	6220800
Convolution	37324800	37324800	0	286891200
Gaussian Pyramid	438110040	438110040	0	2838231226
DOG Pyramid	13820160	0	0	176898096
Gradient & Rotation Pyramids	66288005	24876180	8292060	265345968
Histogram	4600	3576	2	13010
Extrema Refinement	92	102	3	1285
Keypoint Detection	977237	774713	2184	1724135010
Descriptor Extraction	4524956	2249352	300	10798360
Full Run	529942750	469143365	8296348	5030656822

**Table 1.** Recorded flop counts for our implementation, for a sample 1080p image.

execution. This makes it much cheaper for use in continuous image feeds or videos.

Finally, we fix many SIFT parameters in place as constants in order to allow better static memory allocation and constant folding.

## Gaussian Kernel Convolution

The convolution function is one of the main building blocks of our SIFT implementation. It gets called several times to generate the Gaussian pyramid, which is, computationally and time-wise, the main bottleneck in our implementation. And therefore, optimizations to this function promise the biggest payoff.

The main goal of the function is to blur an image by applying a 2D-convolution using a 2D Gaussian kernel. In our baseline implementation, we made use of the separability of the Gaussian filter. Due to this separability, we could split the 2D-convolution into two 1D-convolutions using 1D Gaussian kernels by first filtering the image horizontally and in a second step vertically. In our implementation, the 1D-convolution for the horizontal row filter can be described as

$$g_{i,j} = \sum_{k=0}^{K-1} p_{i-\frac{K}{2}+k,j} * ker_k \quad (7)$$

Where  $p$  is the input image, and  $ker$  is the 1D Gaussian kernel. This gets applied to every

pixel in the input image. The vertical column filter can be described as

$$f_{i,j} = \sum_{k=0}^{K-1} g_{i,j-\frac{K}{2}+k} * ker_k \quad (8)$$

We used the horizontal row filter only and just transposed its output. This allowed us to reuse the same filter function for the vertical part. After the second row filter, the results get transposed again.

For our standard-C optimizations, we increased instruction-level parallelism by using accumulators and unrolling wherever possible. We also applied some tricks, like scalar replacement, to overcome compiler limitations. In our best version, we managed to achieve up to 2x improvement in performance.

We further optimized our implementation using AVX intrinsics. Our best performing version applies the 1D convolution to 8 pixels at once. Further, we made use of FMAs to calculate the sums in equation 7 and 8. This way we managed to achieve a performance increase of more than 5x compared to the baseline.

Due to our measurements showing problems with split loads, we also experimented with replacing the inner moving window by a batched application. However, the shuffling required to replace the moving window gave an overall worse performance penalty than the split loads

did. We also experimented with other blocking and unrolling factors, but were not able to get further performance improvements.

## Gradient and Rotation Computation

One of the bottlenecks we found during profiling was the calculation of the gradient and rotation pyramids.

The calculation of the two pyramids involves differences on a given row  $r$  and column  $c$  in the form of two temporary variables  $t1 = g(r - 1, c) - g(r + 1, c)$ ,  $t2 = g(r, c - 1) - g(r, c + 1)$  where  $g$  is some Gaussian filtered image from the Gaussian pyramid and  $g(r, c)$  a pixel at row  $r$  and column  $c$ .

Due to the fact that for each row and column we look at the row (and column) above and below (resp. to the left and to the right) of it, in our first implementation we used a function to get the pixel at a given position with border clamping. The naive implementation of this function included branching and a worst case of eight conditional checks.

In a first step of our Standard-C optimization, we were able to get a performance boost by reducing the worst case checks from eight to a constant amount of four. We also unrolled an outer loop of three iterations and prevented recalculation of variables which were recyclable. This led to a performance increase of more than 2x.

For the AVX2 implementation we then had to come up for a solution that worked with border clamping. We decided to calculate the border as we have done before and only parallelize the middle of the image. Since the calculations also made use of the `atan2` function a lot, and there was no intrinsic for that, we also implemented an inline method using AVX2 intel intrinsics which we called `eth_mm256_atan2_ps`. Thanks to this implementation, we were able to get an approximate performance increase of about 10x

in total.

## Vectorising atan2

We implemented an AVX2 vectorized version of the `atan2` function, which was mainly used in the Gradient and Rotation Pyramid Computation. Our implementation is able to take `__m256` float vectors  $x$  and  $y$  as input and compute the eight corresponding values in parallel. Difficulties regarding branching in the `atan2` function were overcome by calculating and applying vector masks instead.

## 4. EXPERIMENTAL RESULTS

In this section we detail our performance measurements and discuss how our changes affected the overall runtime and performance of our implementation.

### Experimental Setup

Our measurements were performed on a machine running an Intel Core i7-8700K CPU with a fixed clock at 3.7GHz, with TurboBoost disabled. This model of the CPU is part of the Coffee Lake series and has a 6x32 KB 8-way L1-cache, 6x256 KB 4-way L2-cache, and a 12 MB 16-way shared L3 cache.

Unless otherwise stated, we used ICC 19.1.1.217, with `-g -O3 -mfma -mavx2 -march=skylake -flto -ffast-math -fno-unsafe-math-optimizations` for optimisation flags. We used input images in sizes of 240p, 360p, 480p, 720p, 1080p, 2160p, and 4320p.

### Results

As shown in [Figure 1](#) we managed to achieve an overall speedup factor of about 4x over the reference implementation. This is with speedups of over 5x for the gaussian kernel convolution as shown in [Figure 2](#), and of about 10x for the gradient and rotation pyramids, as shown in [Figure 3](#). As shown in [Figure 4](#), runtime scales

linearly with the size of the image, with diminishing effects as the image size increases. The domination of the gaussian kernel convolution over the rest of the algorithm is clearly shown in [Figure 6](#).

During evaluation we noticed the following interesting factors: for our baseline implementation, GCC produced the fastest code, whereas for our fully optimised implementation, ICC produced the fastest code. For the optimised implementation, changing compiler flags – such as adding `-flto` or `-fno-tree-vectorise` – only minimally impacted runtime, on the level of measurement noise. Aligning memory to pages or even forcing all memory to be paged in ahead of time did not significantly improve runtime. Further measurements and plots detailing all of these comparisons can be found in our repository[5].

The Intel VTune profiler showed that our gaussian kernel convolution was primarily suffering from performance penalties resulting from split loads – floats not aligned with vector register boundaries. This is due to a moving window pass in the inner loop, as mentioned in [section 3](#).

## 5. CONCLUSIONS

In this paper we implemented a high performance version of the SIFT algorithm that can deliver results for 1080p full HD images in real-time. This allows analysis of direct high resolution video streams to detect and track objects as they move around the image. This tracking can be used for camera focus adjustment, computer vision in robotics contexts, and other automated recognition systems.

The biggest bottlenecks in the SIFT algorithm are by far the Gaussian kernel convolution and, to a lesser extent, the generation of the rotation and gradient pyramids. In particular, the Gaussian kernel convolution becomes increasingly dominant as the size of the input image increases.

While a large part of the kernel convolution can be vectorised, a big hindrance is the moving window over the kernel, which causes unaligned memory access and thus many split loads that slow down the register filling. We attempted to circumvent this by prefetching and shuffling as required instead, but this resulted in overall worse performance as cross-lane shuffles are expensive.

Overall, using basic C and AVX optimisations, we managed to achieve a speedup of approximately 4x over the baseline implementation, and of up to 10x in select parts of the algorithm.

The source code for ethSIFT can be found under the zlib license on GitHub:

<https://github.com/shinmera/ethsift>.

## 6. FUTURE WORK

We think it might be possible to replace the Gaussian kernel convolution with an FFT approach to generate the blurred images instead. Whether this would result in improved performance over a fully optimised kernel convolution implementation is not entirely clear to us at this point though.

SIFT steps that are not on the hot path could also be improved further – such as by fusing consecutive additions with FMAs – though we do not see a large benefit to doing so, as the time is massively dominated by the Gaussian convolution and rotation/gradient computations.

Finally, the generation of the pyramid levels could be distributed onto multiple processors relatively easily, as many levels are independent.

## 7. CONTRIBUTIONS OF TEAM MEMBERS

**Nicolas** Implementation of performance and runtime measurement systems, analysis and optimisation of memory allocations and layout,

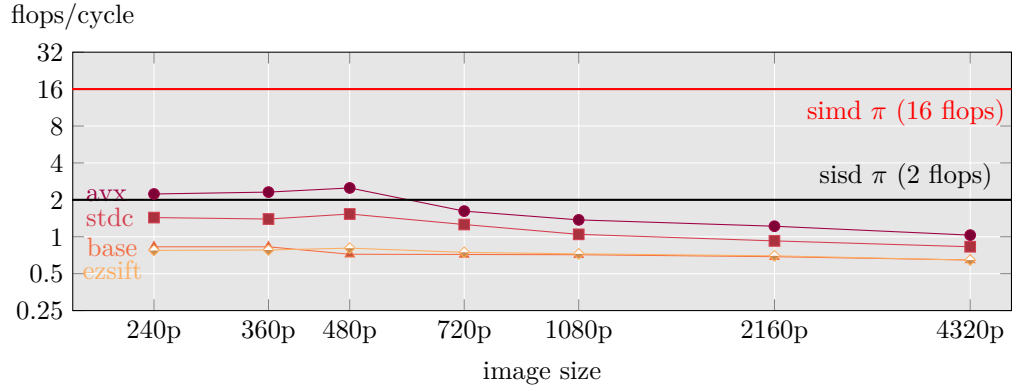


**Fig. 1.** Performance comparison of our optimisation steps for the whole algorithm

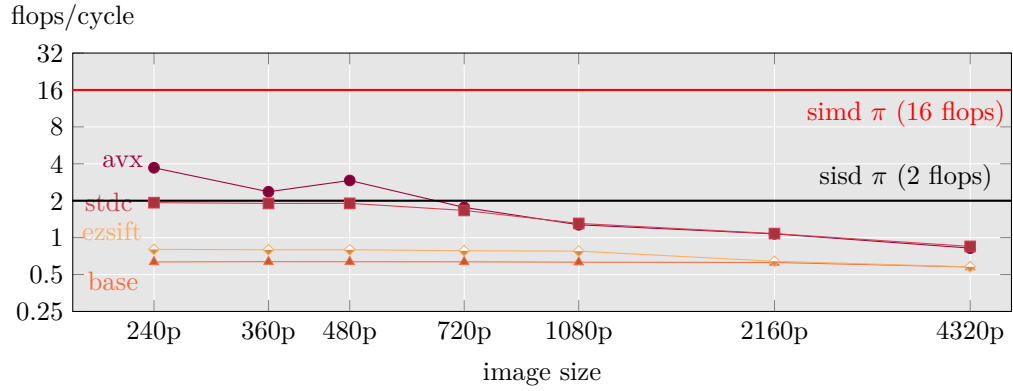


**Fig. 2.** Performance comparison of our optimisation steps for the gaussian kernel convolution

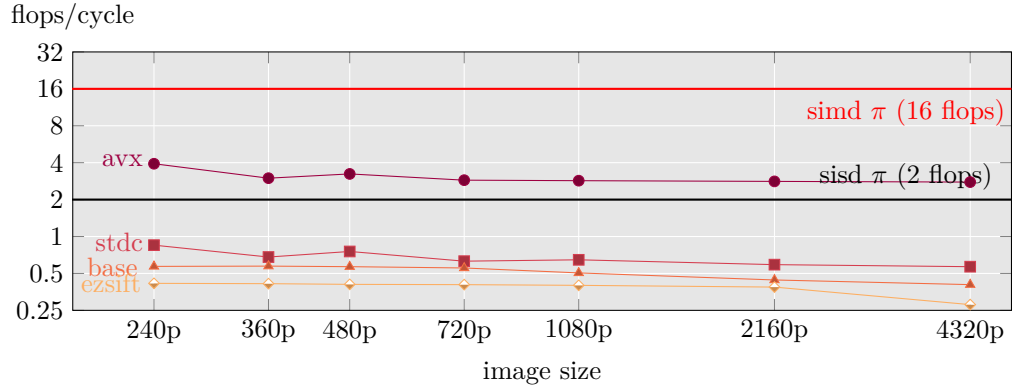


**Fig. 3.** Performance comparison of our optimisation steps for the gradient and rotation pyramids

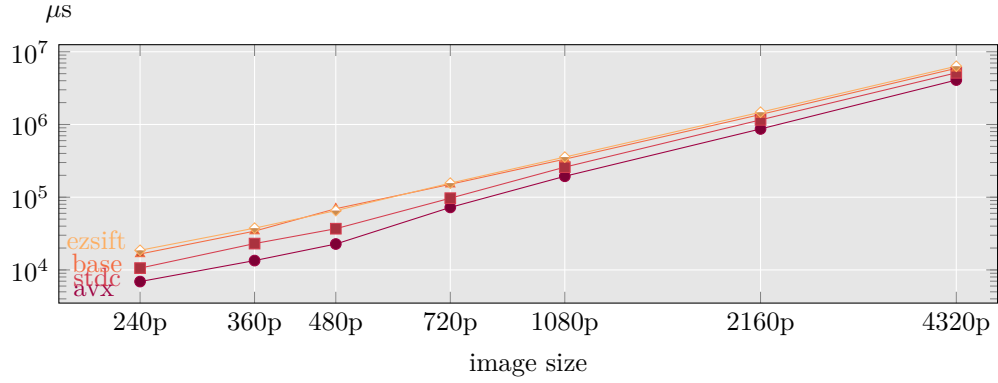


**Fig. 4.** Runtime comparison of our optimisation steps for the whole algorithm

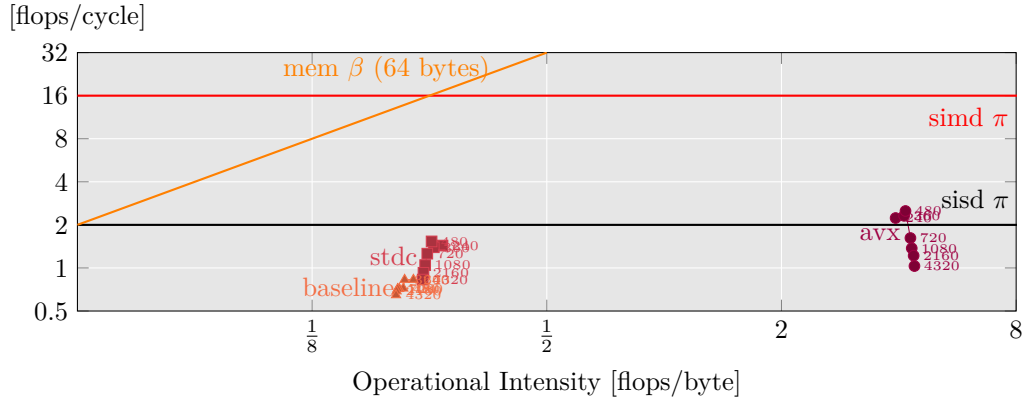


**Fig. 5.** Roofline plot of our optimisation steps for the whole algorithm

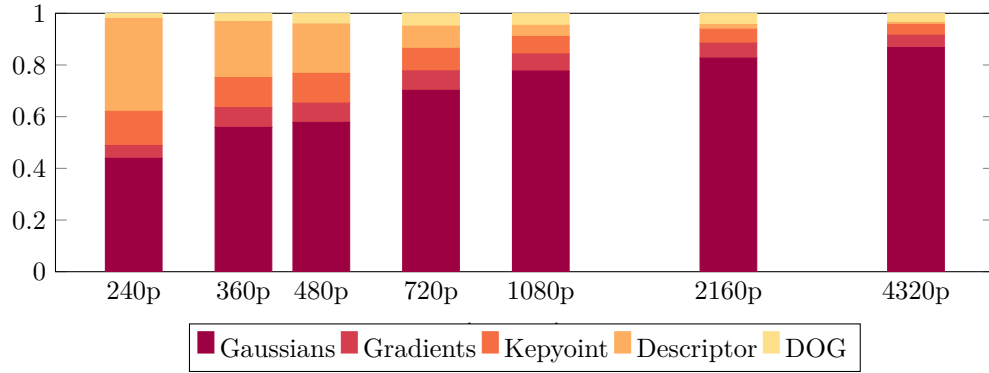


**Fig. 6.** Relative runtime of individual algorithm steps over input size. Histogram computation and extrema refinement are not included, as they are insignificant in runtime.



optimised keypoint detection and histogram computation, helped Jan with analysis and optimisation of the gaussian kernel convolution, as well as with the cycle and memory counters.

**Zsombor** Base implementation of Gaussian pyramids, Kernel generation, Histograms, Compute Keypoints, large amount of tests and measurement methods. Optimized Rotation/Gradient Pyramids & Difference Pyramids. Wrote a large part of our matplotlib-based plotting library. Performed macro cross-compiler analysis. Implemented initial flop counting system along with Costanza.

**Jan** Implementation of flop and memory counting system, base implementation of keypoint detection and extrema refinement, implemented and optimized gaussian kernel convolution, implemented and generated roofline plots, which can be found on our GIT Repository, helped writing tests for ethsift functions, helped Zsombor and Costanza with micro analysis and macro cross-optimisation analysis.

**Costanza** Base implementation of Difference of Gaussian, Gradient and Rotation pyramids, with the relative tests. Optimised Extrema Refinement and Descriptor Extraction. Performed micro analysis and macro cross-optimisation analysis. Contributed to the plot design of Zsombor's plotting library. Implemented initial flop counting system along with Zsombor, and checked for the correctness of Jan's final counting system after every optimisation step.

## References

- [1] David G Lowe. Distinctive image features from scale-invariant keypoints. *International journal of computer vision*, 60(2): 91–110, 2004. URL <https://www.cs.ubc.ca/~lowe/papers/ijcv04.pdf>.
- [2] David G Lowe. Object recognition from local scale-invariant features. In *Proceedings of the seventh IEEE international conference on computer vision*, volume 2, pages 1150–1157. Ieee, 1999. URL <https://www.cs.ubc.ca/~lowe/papers/iccv99.pdf>.
- [3] Guohui Wang. ez sift: An easy-to-use standalone sift library written in c/c++. URL <https://github.com/robertwgh/ezSIFT>.
- [4] Opencv, the open computer vision library. URL <https://opencv.org/>.
- [5] N Hafner, Z Kalotay, C Improta, and J Leutwyler. ethsift: an optimised, pure-c implementation of sift, 2020. URL <https://github.com/shinmera/ethsift>.
- [6] Phaneendra Vinukonda. A study of the scale-invariant feature transform on a parallel pipeline. 2011. URL [http://digitalcommons.lsu.edu/cgi/viewcontent.cgi?article=3720&context=gradschool\\_theses](http://digitalcommons.lsu.edu/cgi/viewcontent.cgi?article=3720&context=gradschool_theses).